Chapter 4
Motion Observation and Experimental Results

This chapter details the experiments used to choose the best data fusion point (Ω_C) to obtain the full frequency measure of the ships velocity, $\boldsymbol{V_E}$, and its position, $\boldsymbol{\eta_E}$. The first experiment investigates properties of the vertical NED acceleration and different methods available to obtain the merged vertical velocity, $\boldsymbol{V_E^Z}$ and merged position, Z_E. The second experiment investigates properties of the data acquisition system on shore, without the ADCP in order to validate the data fusion point of the velocity and position data.

4.1 Vertical Motion

4.1.1 Study of the Acceleration

The intent of the experiment is to observe the vertical NED acceleration, A_Z, implement different integration methods and choose the most suited approach to compute the corresponding vertical velocity and position. The IMU is the only instrument in the data acquisition system providing information about vertical motion. The experiment takes place in a machine shop and consists of mounting IMU, tilt sensor and TCM2 compass on a level plate (Figure 31).

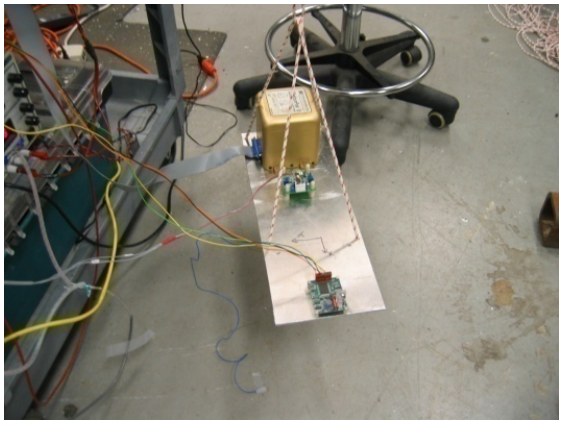

Fig. 31 Vertical motion experiment setup.

The plate is leveled and tethered to the extremity of a 1.03m rigid lever. The middle of the lever is connected to a gearbox itself attached to a rotating engine.

C. Gelin: A Low-Cost, High Rate Motion Measurement System, NAMESS 1, pp. 37–60.
springerlink.com

The extremity of the lever runs on circular trajectories of 0.515m radius at different speeds. The test consists of six sets of vertical roundtrip periods of approximately 5, 10, 15, 20, 25 and 35 s, each lasting about 10 minutes (Figure 32). The speeds are manually set in an automatic manner using the speed variator of the rotating engine.

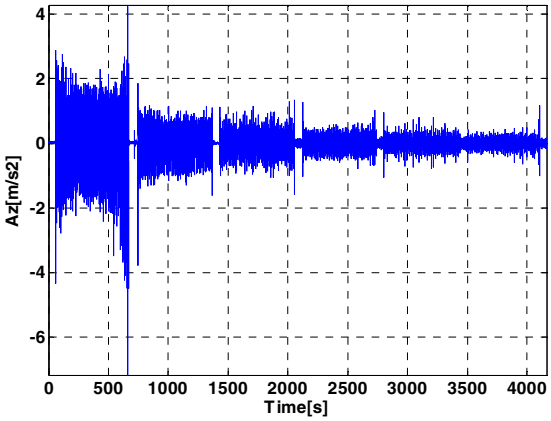

Fig. 32 Vertical motion experiment: raw vertical acceleration A_z.

Filtering of raw data is necessary before concluding on the systems' performance. The test is conducted in a noisy environment, with loud air conditioning on and heavy machinery, some of it running during the test, leading to perturbation on the data unrelated to the actual motion of the plate. In addition, even though the cord holding the plate was chosen to hardly extend, a low frequency perturbation still remains, likely due to the stretch of the cord. Since those perturbations are less likely to exist at sea, the filtering is taking into account the wave frequency range (0.03 – 0.3Hz). A 2nd order bandpass Butterworth filter with cutoff frequencies 0.01 and 0.4Hz is found to be the most suited preserving motion and filtering noise (Figure 33). Figure 33 shows on the left side, a close up on the motion using the PSD of A_Z, from top to bottom for the set 1 (a), 3 (c) and 5 (e) of periods about 5, 15 and 25 s. On the right side of the figure, the close up on the effect of the filtering for the set 1 (b), 3 (d) and 5 (f) is presented. The signals pre-filtering are in red while in blue are the filtered signal with a 2nd order bandpass Butterworth, cutoff frequencies 0.01 and 0.4Hz. All filters used in this book are Butterworth filters as they are typical and Elliptic filters may have been used as well.

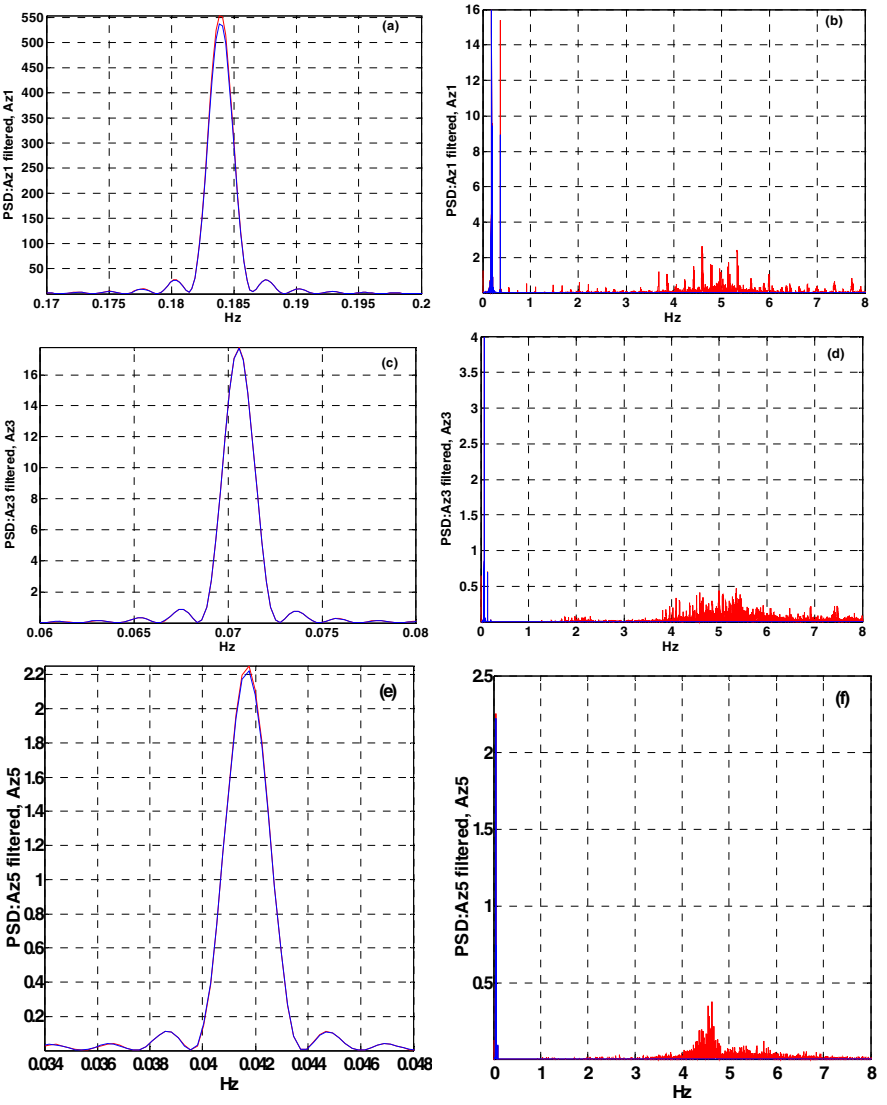

Fig. 33 A_Z spectrum from top to bottom for the set 1 (a), 3 (c) and 5 (e) of periods about 5, 15 and 25 s (left side) and filtering effect on the signal (right side) for the set 1 (b), 3 (d) and 5 (f).

A close up, in time domain, of three sets of period 5 (a), 15 (b), and 25s (c), is shown in Figure 34. The black signal represents the recorded data and the red signal the filtered data with a 2nd order bandpass Butterworth with cutoff frequencies 0.01 and 0.4Hz. Figure 34 highlights the filtering necessity as higher the period of the set, higher the noise and lower the signal to noise ratio.

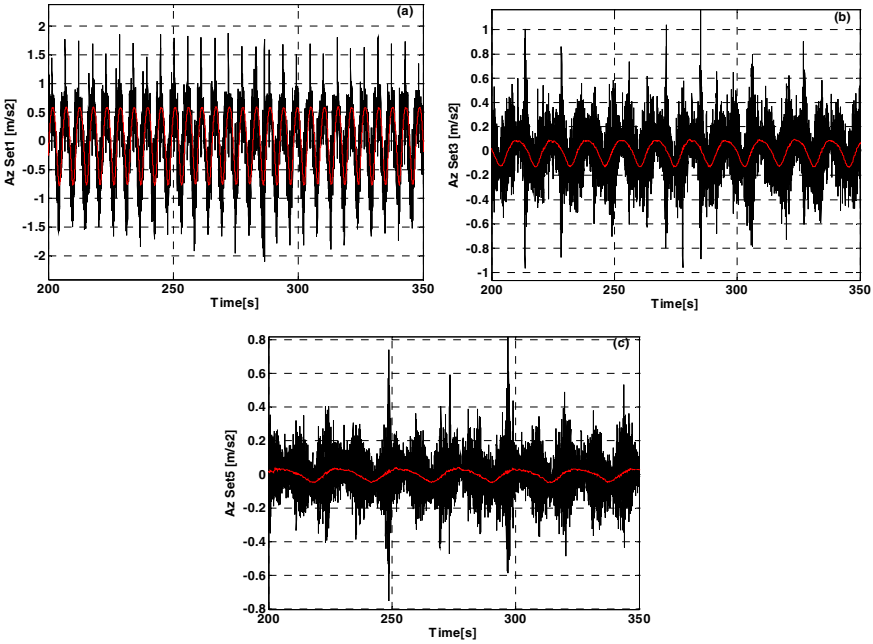

Fig. 34 Measured and filtered acceleration for periods about 5 (a), 15 (b) and 25s (c). Acceleration measurements are in black while filtered accelerations are in red.

The period of the movement is isolated to recreate the expected motion (Figure 35).

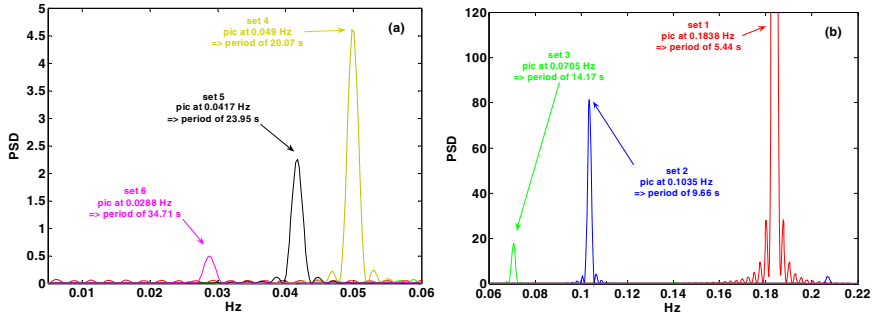

Fig. 35 A_z PSD for the set 1, 2 and 3 (b) of periods about 5, 10 and 15 s, and for the set 4, 5 and 6 (a) of periods about 20, 25, and 35 s.

The expected motion (S_{Theo}) is simulated using a sinusoidal signal with the period corresponding to the set (T_{SET}) and the amplitude according to:

$$\bar{S}_{Theo} = \frac{(2\times\pi\times 0.515)}{T_{SET}}. \tag{34}$$

The expected motion is going to be compared to the measured signal using crosscorrelation and an agreement of more than 90% is considered acceptable. Figure 36 is a close up on the sets 1 (a), 3 (b) and 5 (c) with the expected motion in red, the system acceleration in blue, and the difference between the signals in black. The black signal's standard deviation represents the acceleration signal's accuracy.

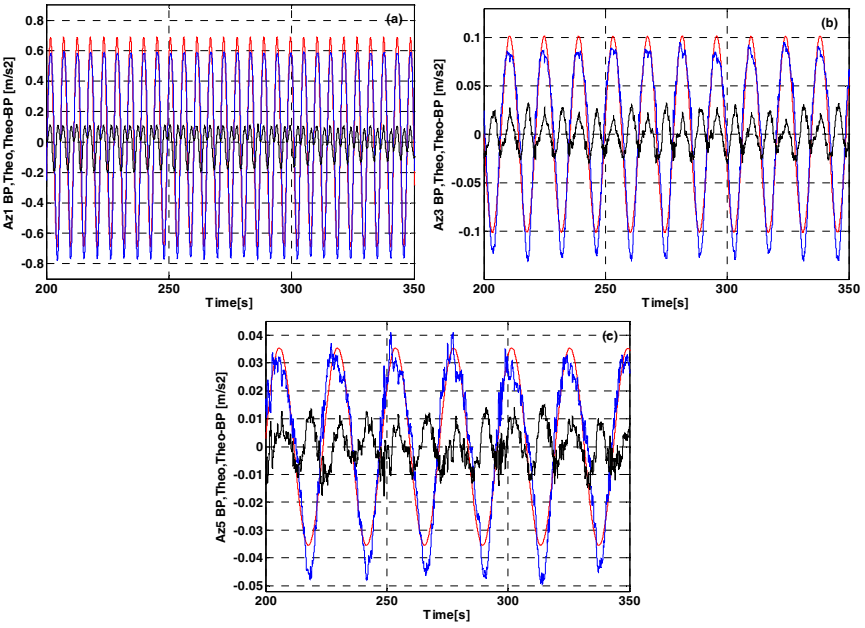

Fig. 36 Close up of the acceleration for the set 1 (a), 3 (b) and 5 (c) of periods about 5, 15 and 25s with the expected motion in red, the system acceleration in blue and the difference between the signals in black.

The black signal's behavior emphasizes that the slower the motion, the smaller its resulting standard deviation, the higher the agreement between expected and obtained signal. The black signal's standard deviation is respectively 9.6 ± 8.5891 cm/s^2 (taking into account the specification of the instrument), 1.5239 ± 1.2652 cm/s^2 and 0.66908 ± 0.44294 cm/s^2. According to a crosscorrelation calculation conducted, they agree respectively at 98%, 97.7% and 96% with a delay of 0.015s each.

4.1.2 Velocity Calculations

The IMU has low frequency noise like most accelerometers and since the integration process amplifies significantly the low frequencies, different methods are evaluated that focus on minimizing the low frequency noise. Three methods are evaluated for obtaining vertical velocity from acceleration data.

The first method integrates numerically the acceleration measurement using the cumulative summation (Matlab function *cumsum*) of the signal over the sampling frequency. The low frequency contamination is then removed using the Matlab function *detrend* considering the low frequency contamination from the integration as a linear trend.

The second method numerically integrates the acceleration measurement then applies a high-pass filter to the obtained velocity signal.

The last method applies the data fusion technique. The concept behind using this method is that the IMU, which is assumed accurate only at high frequencies, is merged with an ideal signal containing no low frequencies (null signal) to remove the low frequency noise from the integration.

This sub-section describes each one of the 3 aforementioned techniques. In each of the sub-sections, the red signal represents the expected motion, the blue the system's motion, and the black the signals difference. The black signal's standard deviation is an indicator of the velocity signal's accuracy.

4.1.2.1 Vertical Velocity Resulting from Integrating Acceleration and Removing the Induced Trend

A close up of the effect of integrating the acceleration (using the Matlab function *cumsum*) and using a low frequency contamination removal function (*detrend*) is shown for the sets 1 (a), 3 (b), and 5 (c) in Figure 37. Detrending a signal refers to applying the matlab function *detrend* to the signal.

The red signal represents the expected velocity obtained by integrating the expected acceleration, the blue signal is obtained integrating then detrending the obtained acceleration and the black signal is the difference between expected and obtained velocities. The black signal's standard deviation is respectively 6.27 cm/s, 2.3 cm/s and 1.9 cm/s. The lower the standard deviation of the black signal the better the method since the goal of the method is matching obtained signal with expected motion. This method fails at removing all low frequency perturbations leading to the need for another method based on a high-pass filter use.

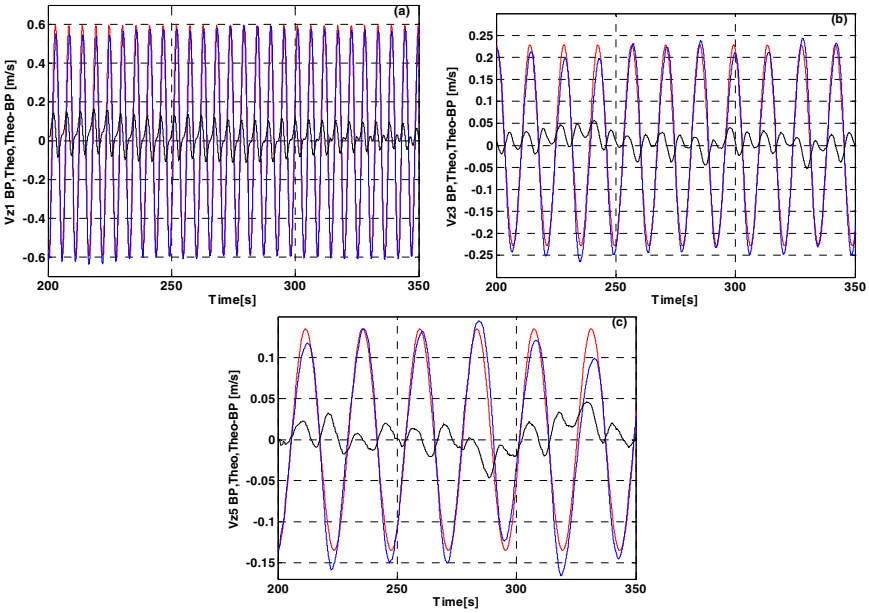

Fig. 37 Difference, in black, between the expected velocity V_Z, red, and the obtained velocity using the *detrend* function on the integrated acceleration in blue for the set 1 (a), 3 (b) and 5 (c).

4.1.2.2 Vertical Velocity Resulting from High-Pass Filtering the Integrated Acceleration

A close up of the effect of high-pass filtering on the integrated signal is shown for sets 1 (a), 3 (b), and 5 (c) in Figure 38. The expected velocity is in red, the blue signal is the velocity resulting from integrating then high-pass filtering the obtained acceleration and the black signal is the difference between expected and obtained velocities. A 4^{th} order Butterworth high-pass filter with cutoff frequency of 0.021Hz is found to be the most suited filter to minimize phase delay and eliminate low frequency perturbation due to the integration process. The Butterworth filter is selected because typical and an Elliptic filter could also have been used. The black signal's standard deviation is respectively 6 cm/s, 1,8 cm/s and 1.3 cm/s which is overall lower than the standard deviations obtained through the first method. This method fails at removing all perturbations at low frequency leading to the blue signal following a trend different than the red signal. But the method provides better results considering the standard deviation of the black signal than the first method involving use of the *detrend* Matlab function.

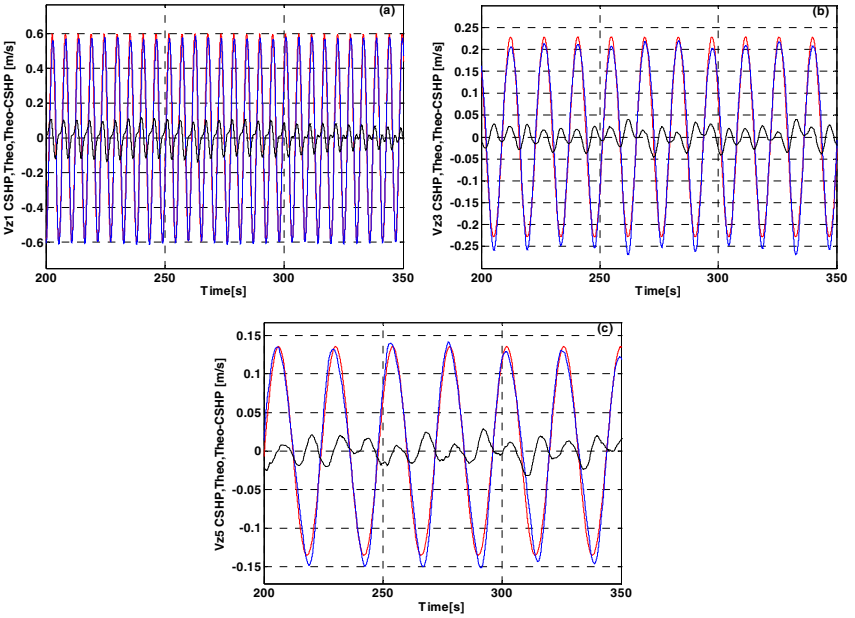

Fig. 38 For the sets 1 (a), 3 (b) and 5 (c), velocity obtained using a high-pass filter on the integrated acceleration, in blue, plotted against the expected velocity V_Z, in red. The difference between the two signals is in black.

4.1.2.3 Vertical Velocity Using the Data Fusion Technique

Results for the data fusion method is shown for the sets 1 (a), 3 (b), and 5 (c) in Figure 39. The red signal is the expected velocity, the blue signal the obtained velocity resulting from the data fusion technique, and the black signal the difference between expected and obtained velocities. The IMU, which is assumed accurate only at high frequencies, is merged with a null signal at low frequency by replacing V_{LF}^{Z} by 0 in (28). The black signal is the difference between expected and obtained velocities. A data fusion point at 1/100Hz is found to be the best compromise to merge IMU with null signal. With this method, the standard deviation of the black signal is respectively 6.9 cm/s, 1.9 cm/s and 1.5 cm/s. Looking at the standard deviation of the black signal for each one of the three methods and since the best method will have the lowest standard deviations, this method is not as satisfying as the second method and better than the first method for the set 3 and 5. This method is selected over the second method because it introduces less delay than using a 4^{th} order Butterworth filter.

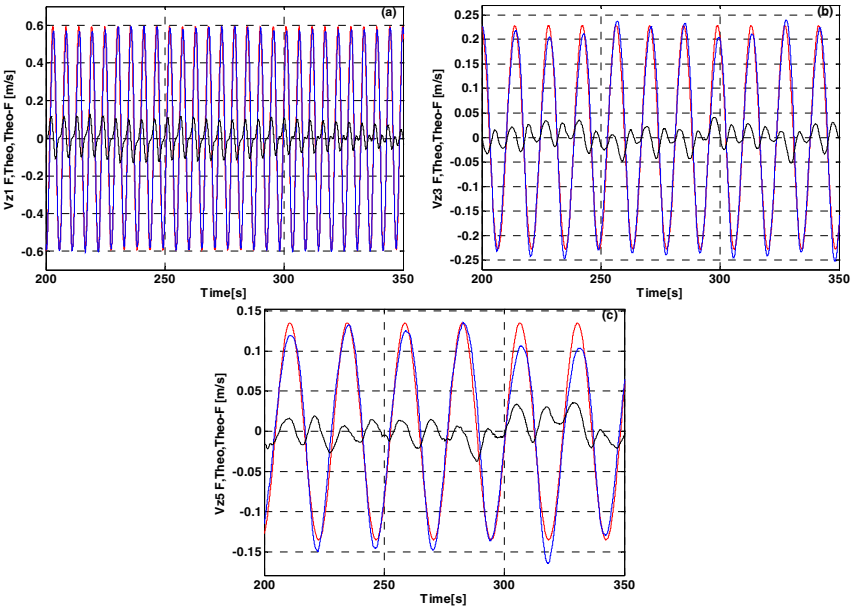

Fig. 39 For the sets 1 (a), 3 (b) and 5 (c), velocity obtained by data fusion, in blue, plotted against the expected velocity V_Z, in red. The difference between the two signals is in black.

4.1.3 Vertical Position Calculations

Two methods are applied to obtain the vertical position from obtained velocity data. The first method is to integrate the velocity estimates at fixed time steps using the cumulative summation and to high-pass filter the result. The second method is to merge the velocity obtained in 4.1.2 with a null signal at low frequency by replacing $Z_{,LF}$ by 0 in (28). This sub-section describes each of the two aforementioned techniques. In each of the sub-sections the red signal represents the expected motion, the blue the system motion, and the black the difference between the two. The standard deviation of the black signal is used to quantify the accuracy of the position signal.

4.1.3.1 Vertical Position Calculated Using the High Pass Filtered Integrated Velocity

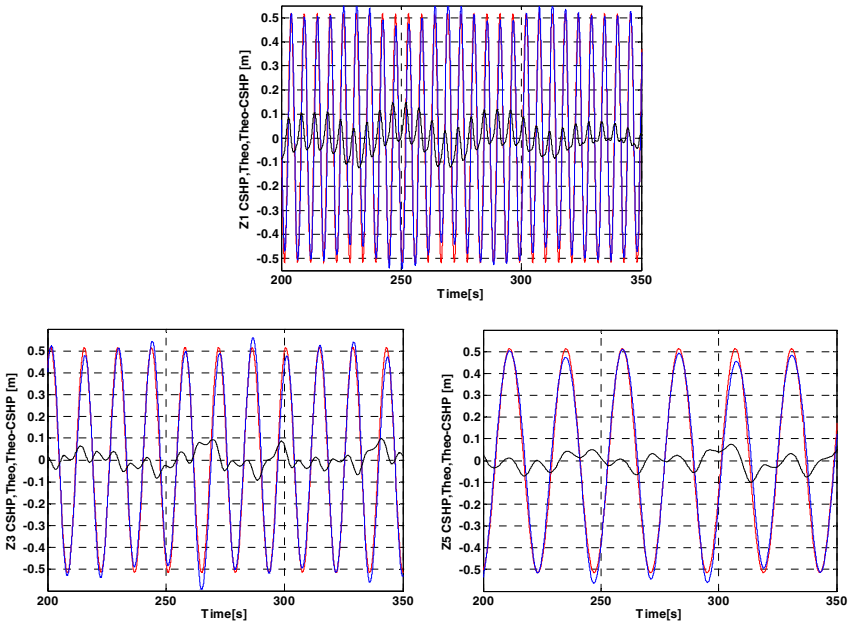

Fig. 40 For the sets 1 (a), 3 (b) and 5 (c), position obtained using a high pass filter on the integrated velocity, in blue, plotted against the expected position Z, in red. The difference between the two signals is in black.

Results obtained using the first method are shown for the sets 1 (a), 3 (b), and 5 (c) in Figure 40. The red signal is the expected position obtained by integrating the expected velocity, the blue signal is the position estimate obtained by integrating then high-pass filtering the velocity estimates in 4.1.2, and the black signal is the difference between expected and obtained position. A 4^{th} order high pass Butterworth filter with cutoff frequency of 0.021Hz is found to be the most suited filter limiting phase delay and minimizing low frequency amplification due to the integration process. The Butterworth filter is selected because typical and an Elliptic filter could also have been used. The standard deviation of the black signal with the first technique is 4.8 cm, 4.3 cm, and 3.9 cm respectively.

4.1.3.2 Vertical Position Calculated Using the Data Fusion Technique

Results obtained using the second method are shown for the sets 1, 3, and 5 in Figure 41. The red signal is the expected position, the blue signal the position obtained using the data fusion technique with the velocity obtained in 4.1.2 merged with a null signal at low frequency by replacing $Z_{,LF}$ by 0 in (28), and the black signal is the difference between expected and obtained position. A cutoff frequency of 1/50Hz for the data fusion is found to be the best compromise to

merge the obtained velocity with the null signal. The black signal's standard deviation is respectively 6.7 cm, 5.6 cm and 7.6 cm. Although this method provides a high standard deviation measurement for the black signal, it is selected for the processing of the vertical position moving forward since it is compatible with real time applications.

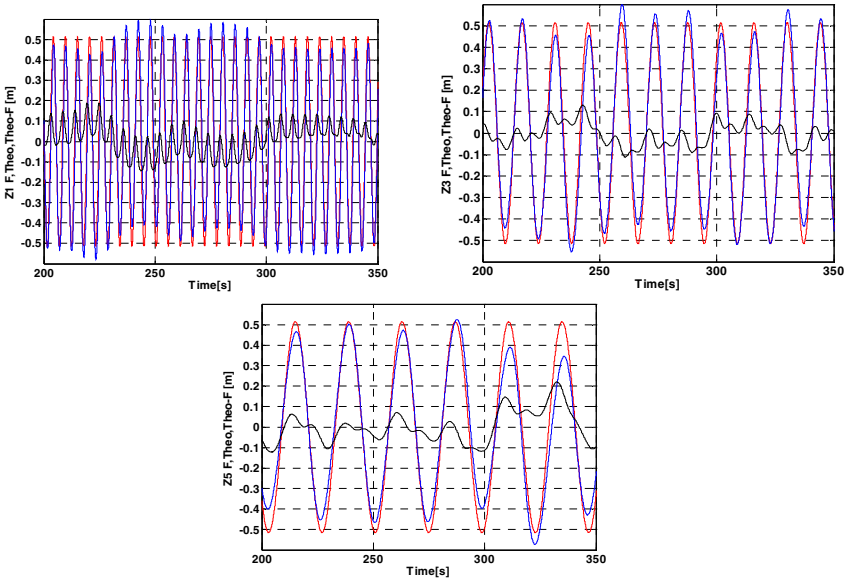

Fig. 41 For the sets 1 (a), 3 (b) and 5 (c), position obtained by data fusion, in blue, plotted against the expected position Z, in red. The difference between the two signals is in black.

4.2 Data Acquisition System Lab Testing

The following section presents the experiments used to investigate and optimize the data fusion between the IMU and GPS signals. This is accomplished by first observing the sensors outputs then selecting a frequency for the data fusion and finally verifying the merged signal obtained is combining the comple-mentary region of the two sensors. The complete data fusion process used to accurately determine the position and velocity signals

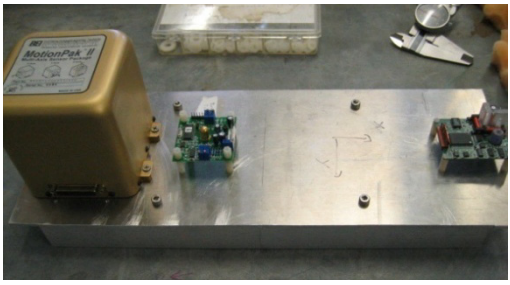

Fig. 42 IMU, tilt sensor, and TCM2 compass attached to a rigid plate attached to the cart.

consists of two data fusions: the first data fusion process, involving the IMU acceleration and the GPS velocity measurement leads to a full frequency assessment of the velocity measurement. This frequency for the data fusion is selected so that at frequencies lower than the cutoff frequency (to be determined) the GPS provides an accurate measure of the system's velocity, and at frequencies above the cutoff frequency the IMU provides an accurate estimation of the velocity. The second data fusion is performed between the merged velocity, obtained from the first data fusion, and the GPS position measurement. Similar reasoning to that used for the first data fusion is applied, i.e. for frequencies lower than the cutoff frequency the position estimate is provided by the GPS, while for frequencies above the cutoff frequency the measure of position is derived from the merged velocity signal.

The experiments take place in an open parking lot to ensure the GPS system has a clear and unimpeded signal. The experimental setup consists in mounting the IMU, the tilt sensor and the compass on a rigid plate that is fixed to a cart (Figure 42) where the rest of the data acquisition system (without the ADCP) is mounted. Once the sensors' signals are acquired, decoded, and synchronized, they are sent to the PC104 logger stack to be saved to the flash drive. These signals are later post processed to find the best frequencies for the data fusions for the evaluated sensors.

During each test the cart is initially stationary for at least two minutes. Because of the lack of automatic motion control, the cart is then moved manually between four spots on the ground that mark the corners of a square with 7.88m leg and the corners pointing towards the four cardinal points. The use of industrial foam and the choice of a cart with large wheels are among the precautions taken to minimize the vibrations caused by the uneven ground. Three trajectories are selected: a square path, a zigzag course and a circle. These trajectories are repeated at least three times each at different speeds. The path of the trajectories, speed and periodicity are selected to test the system's ability to accurately measure the cart motion.

Conventions used in this chapter are as follows:

The GPS position vector is denoted $\boldsymbol{P_{gps}}$ which is composed of X_{gps}, its north-south component, Y_{gps}, its east-west component, and Z_{gps}, its vertical component. Similarly, V_{xgps} and V_{ygps} represent the north-south and east-west velocity components, respectively, and V_{zgps} is the vertical component of the GPS velocity vector, $\boldsymbol{V_{gps}}$:

$$\boldsymbol{P_{gps}} = [X_{gps}, Y_{gps}, Z_{gps}]^{\mathrm{T}}, \tag{35}$$

$$\boldsymbol{V_{gps}} = [V_{xgps}, V_{ygps}, V_{zgps}]^{\mathrm{T}}. \tag{36}$$

Similarity the IMU acceleration vector is defined by:

$$\boldsymbol{A_{IMU}} = [A_x, A_y, A_z]^{\mathrm{T}}. \tag{37}$$

The determination of the data fusion frequency for the data fusion process is based on 4 steps applied to each one of the three trajectories. The steps are as follows:

1) processing of the raw data and selection of the data fusion frequency, 2) Observing the signal spectrum to validate the choice of the data fusion frequency, 3) Observing the crosscorrelation of the low-passed merged and low-passed GPS measurements to quantify their agreement with each other and Step4; calculation of the standard deviation of the merged signal using a high-pass filter to remove any motion contamination (Figure 43).

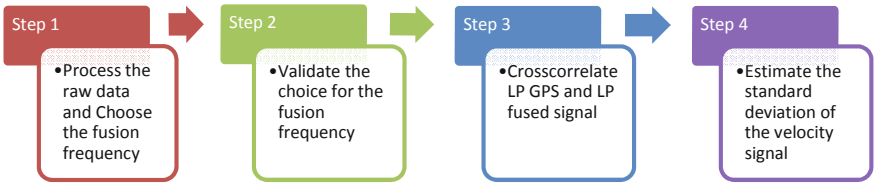

Fig. 43 Methodology used to find the data fusion frequency between IMU and GPS measurement to recover full frequency estimate of the system's position and velocity.

4.2.1 Step 1: Processing of Individual Measurements

During this analysis, the DGPS measurements are used to calculate distance travelled and duration for each trajectory. Since the start and end points of each shape are the same, it is possible to evaluate the period, i.e. the track periodicity. This is particularly important for the sensor's data frequency analysis to distinguish the actual motion of the cart from possible perturbations and noise. The first part of this section describes the results from the analysis of the sensor's measurements in the time domain and the second part describes the results in the frequency domain.

The three paths as perceived by the DGPS are shown in Figure 44, Figure 45 and Figure 46. The first trajectory follows the 7.88m legs of the square starting at the coordinates Y= -2 and X= -2 on Figure 44 and going southwest, then southeast, then northeast, and finally northwest.

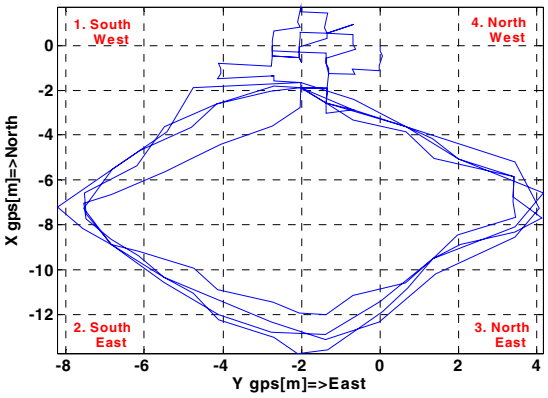

Fig. 44 Square path, as perceived by the DGPS.

The path is repeated four times in approximately three minutes. The first two squares are each completed in approximately 57.8s and the last two in 34.35s. The DGPS reflects the motion of the cart within its 3 meter accuracy. According to the DGPS velocity data, the cart is moving at 0.55m/s during the first two square paths and about twice as fast for the last two, at 0.93m/s. The second path, following the same general square trajectory but proceeding in a zigzag pattern between corners, is repeated four times 90.22s each with a total of a little over six minutes, (Figure 45). The DGPS responded sharply to the sudden change of direction of the cart. According to the DGPS velocity measurement, the cart moves at approximately 0.39m/s.

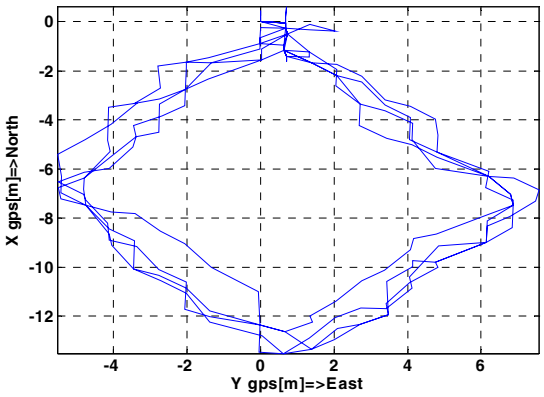

Fig. 45 Square path proceeding in a zigzag pattern between corners, as perceived by the DGPS.

The last path follows a 39m perimeter circle which is repeated five times in approximately six minutes. The fourth circle travelled has an ellipsoidal shape due to the DGPS position's error. The first three circles represent a 39.3m distance travelled in 83s. The ellipsoidal path is 32.83m and is conducted in 64s. Finally, the last circle takes 60.9s to travel 36.29m (Figure 46). The cart swerved less than 3 meters when attempting to manually recreate the same trajectory four times in a row. The DGPS measurements reflect both the cart's swerve and its 3 meters accuracy range.

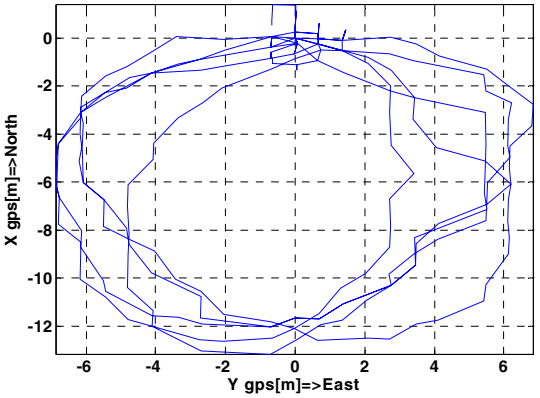

Fig. 46 Circle path as perceived by the DGPS.

The uneven track induced the data acquisition systems to tilt and those angles are measured by the tilt sensor (Figure 47). Although pitch and roll applied to the data acquisition system impacts the IMU accelerometers, these are taken into account in the processing of the IMU acceleration measurement. As an example of that impact, the error induced on the IMU acceleration by tilting is calculated for the first trajectory test. The tilt sensor's roll and pitch measurement of the square path have a mean of -0.4° and -1.275° respectively, with a standard deviation of ± 1.44° and ± 0.93° respectively. At the maximum roll angle, 1.84°, it influences the east component of the acceleration by -0.315m/s^2 and at the maximum pitch angle, 2.2°, the north component of the acceleration by 0.376m/s^2. The tilt sensor's roll and pitch for the three trajectories are shown in Figure 47 and Table 6 presents their mean and standard deviation as well as the influence of the maximum deviation of the data on the IMU east and north component of the acceleration.

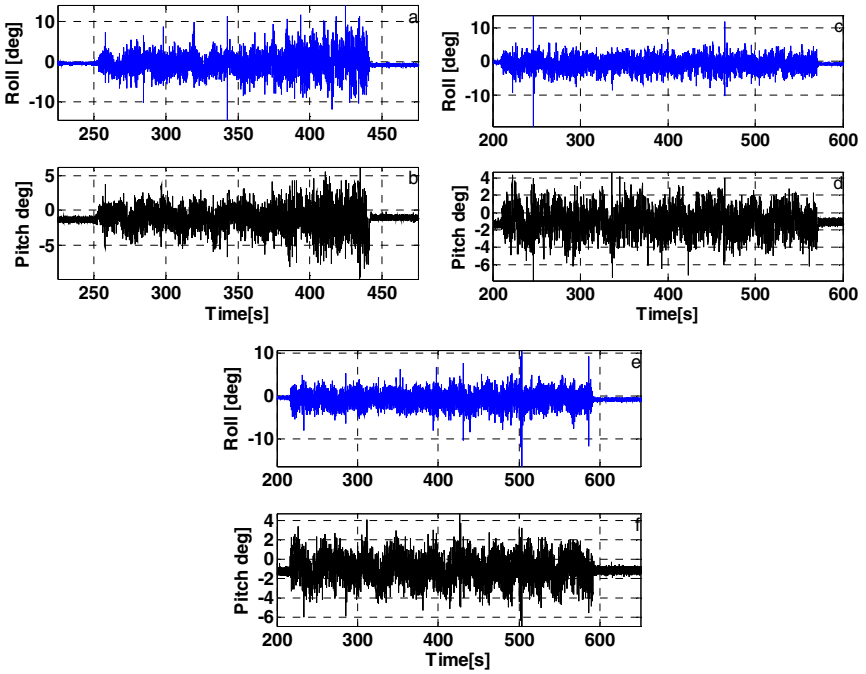

Fig. 47 Roll and Pitch of the cart measured by the tilt sensor during the first trajectory ((a) and (b)), the second trajectory ((c) and (d)) and the third trajectory ((e) and (f)).

Table 6 Mean and standard deviation of the tilt sensors' roll and pitch as well as the influence it could have on the IMU acceleration if not considered for the three trajectories of the on shore test of the data acquisition system.

		Trajectory		
		Square	**Square in zigzag course**	**Circle**
ROLL	Mean [°]	-0.4	-0.631	-0.6321
	STD [°]	± 1.44	± 1.253	± 1.096
	Influence on Ay [m/s^2]	-0.315	-0.3225	1.7281
PITCH	Mean [°]	-1.275	-1.156	-1.165
	STD [°]	± 0.93	± 0.946	± 0.8169
	Influence on Ax[m/s^2]	0.376	0.356	0.3392

The study of the tilts concluded that the cart has rolled 0.55° ± 1.26°, and has pitched 1.19°± 0.89° on average. The second part of the processing of the raw sensor's data is to observe the measurements in the frequency domain. For the study of the signals in the frequency domain, the power spectral density (PSD) of each signal is used. The IMU PSD accelerations are obtained for the three trajectories and shown in Figure 48. The notation *PSD Ax/Ay* means the graph is representing both the PSD of Ax and the PSD of Ay in two different colors.

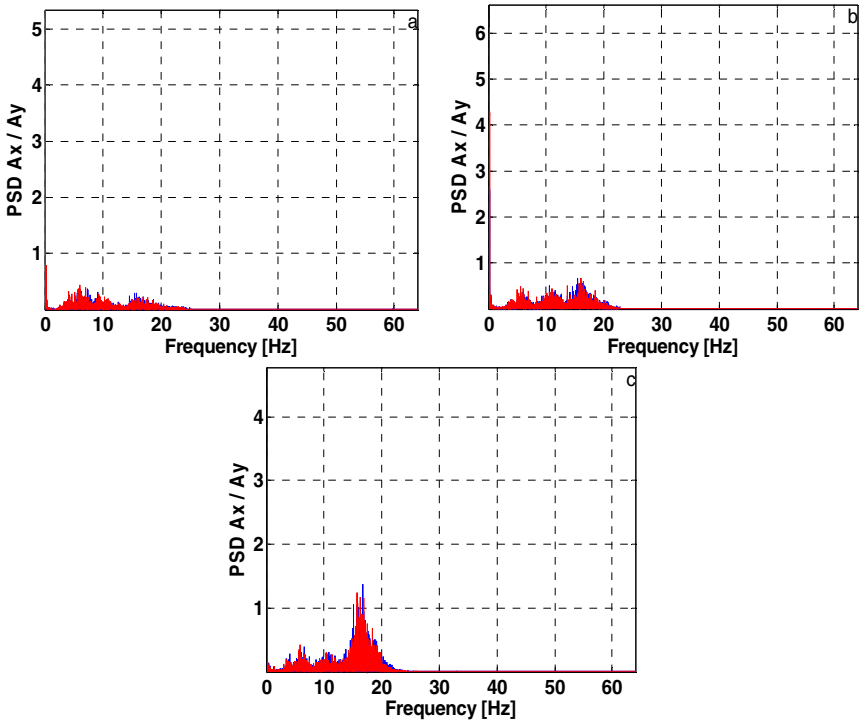

Fig. 48 PSD of the north component, in blue, and the east component, in red, of the IMU acceleration during square trajectory (a), square path by processing in zigzag course (b) and the circle trajectory (c).

Figure 48 shows significant spectral content for frequencies above 2Hz present in the measurements. The Notation PSD Ax/Ay indicates that the plot has both the PSD of Ax and the PSD of Ay represented. The scale is chosen to show the noise starting at 2Hz and most likely coming from the vibration of the cart and from the batteries located nearby the system. These high frequencies are most likely a combination of valuable high frequency component of the IMU measurement and noise from the vibration of the IMU on the cart and from the battery nearby the data acquisition system. Among the noise is valuable high frequency information on the IMU acceleration measurements essential for the data fusion process with the GPS. No low-pass filtering can be applied to the data prior to the data fusion process and high frequency noise is going to be relatively attenuated by the low-pass filter applied at the last stage of the data fusion process. To be aware of the signal to noise ratio of the IMU acceleration measurement, a first order Butterworth low-pass filter with a cutoff frequency at 2Hz is applied to the signals to remove the aforementioned noise at 2Hz and the result can be seen in Figure 49. The plots (a), (d) and (g) [respectively (b), (e), (h) and (c), (f), (i)] shows the north (respectively east and down) component of the acceleration in blue and the signal

after low-pass filtering the noise at 2Hz in red. The signal to noise ratio is approximately 1 to 2. The Butterworth filter is selected because typical and an Elliptic filter could also have been used. The filtering is only done for a better understanding of the frequency distribution of the signal and is not included in the data fusion process.

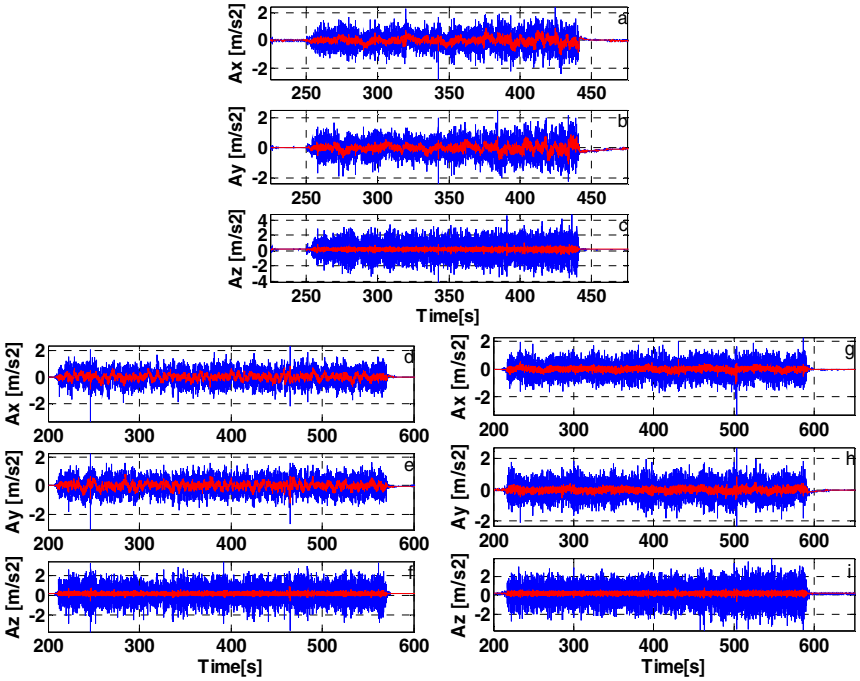

Fig. 49 Influence of frequencies above 2Hz on the IMU acceleration measurements for the three trajectories of the on shore test of the data acquisition system.

Finally, the DGPS position, velocity and the IMU acceleration are studied in the frequency domain to determine the complementary regions of the sensor. The detection of the frequency peak corresponding to the cart's motion, which appears in each one of the signals spectrum, is the first step in observing the complementary regions of the sensors. Figure 50 presents the spectrum of the DGPS position signal (Figure 50.a), DGPS velocity signal (Figure 50.b) and of the IMU acceleration (Figure 50.c) during the first trajectory (square path). The frequency corresponding to the first two square paths is close to 0.015Hz and for the last two squares close to 0.02Hz. Once the frequency peaks corresponding to the cart's motion are detected, around 0.02Hz in this example, the visualization of where the DGPS and IMU measurements have most of their significant spectral content is used to choose the data fusion frequency.

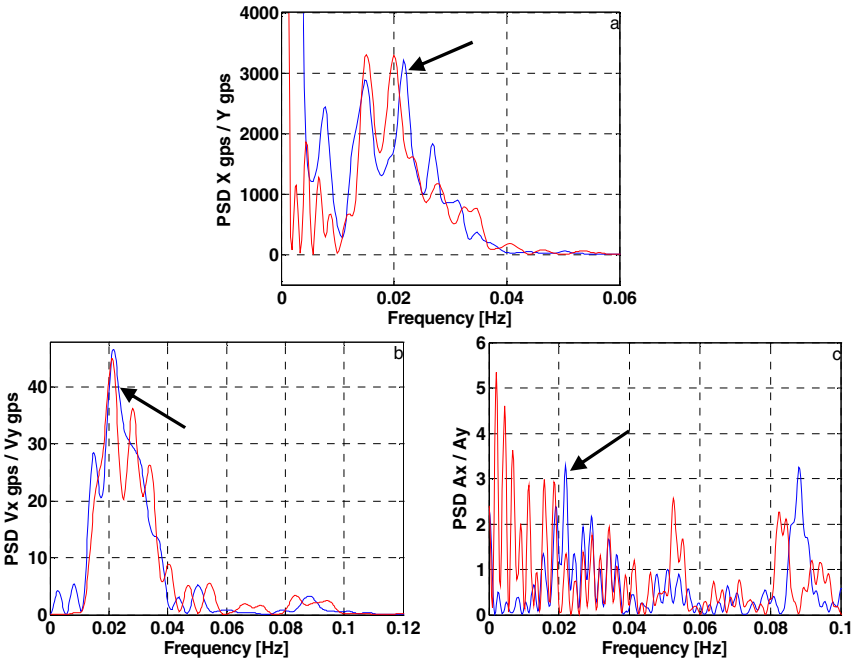

Fig. 50 PSD of the DGPS position (a), DGPS velocity (b) and IMU acceleration (c) for the first trajectory of the on shore test, following a square path. The blue signal corresponds to the north component of the measurement and the red signal to the east component.

The DGPS has most of its significant spectral content around the peak of interest (Figure 50.a and Figure 50.b) corresponding to the cart's motion and almost no significant spectral content at higher frequencies. On the other hand, Figure 50.c shows how the IMU sensed the low frequency motion of the cart, smothered by other frequencies, while still responsive over a frequency range greater than the DGPS. This observation shows the importance of the IMU data being filtered out of the region where the DGPS delivers accurate measurements in order to avoid perturbations on the low frequency estimate of the merged signal. To do so, a 3rd order high pass Butterworth filter with a cutoff frequency at 0.1Hz (Nyquist frequency) is applied to the IMU acceleration measurement prior to the data fusion process. The Butterworth filter is selected because typical and an Elliptic filter could also have been used. The detection for the frequency peak corresponding to the cart's motion is applied for all the trajectories and results are compiled in Table 7.

Table 7 Results from the peaks of frequency detection corresponding to the cart's motion for the three trajectories.

Frequency peak corresponding to the cart's motion [Hz]		Square		Square in zigzag course	Circle
		First two paths	Last two paths		
DGPS POSITION	North Component	0.01489	0.02173	0.01074	0.01318
	East Component	0.015	0.02	0.01074	0.01318
DGPS VELOCITY	North Component	0.01489	0.021	0.01074	0.01245
	East Component	0.01489	0.021	0.01123	0.0127
IMU ACCELERATION	North Component	0.015	0.021	0.01074	0.012
	East Component	0.015	0.021	0.01074	0.012

The study of the spectrums for the other two trajectories leads to similar observations as in Figure 50 where the DGPS has most of its significant spectral content just after the peak of interest corresponding to the cart's motion. These observations suggest that the complementary regions of the sensors overlap around 0.05Hz, which is used as the data fusion point.

4.2.2 Step 2: Validate the Choice for the Data Fusion Frequency

As aforementioned, the IMU acceleration measurement is high-pass filtered prior to the data fusion process and the data fusion point is selected at 0.05Hz. Figure 51 shows the diagram of the first data fusion process.

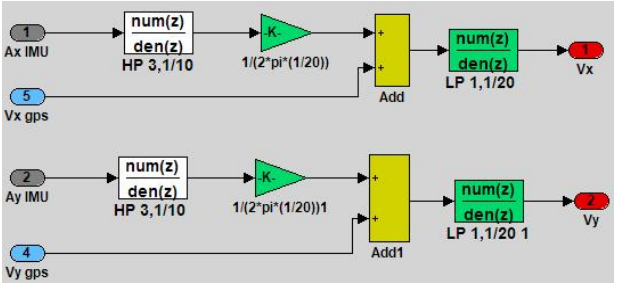

Fig. 51 Data fusion diagram between the IMU acceleration data and the DGPS velocity measurements in order to obtain the enhanced velocity estimate.

The data fusion frequency validation is applied observing the signals though key sequential steps, depicted in Figure 51. The frequency domain is selected for that investigation. Figure 52 shows the results of this analysis for the north component of the DGPS velocity and the north component of the IMU acceleration during the square maneuver. The same process is applied for all the signals and trajectories.

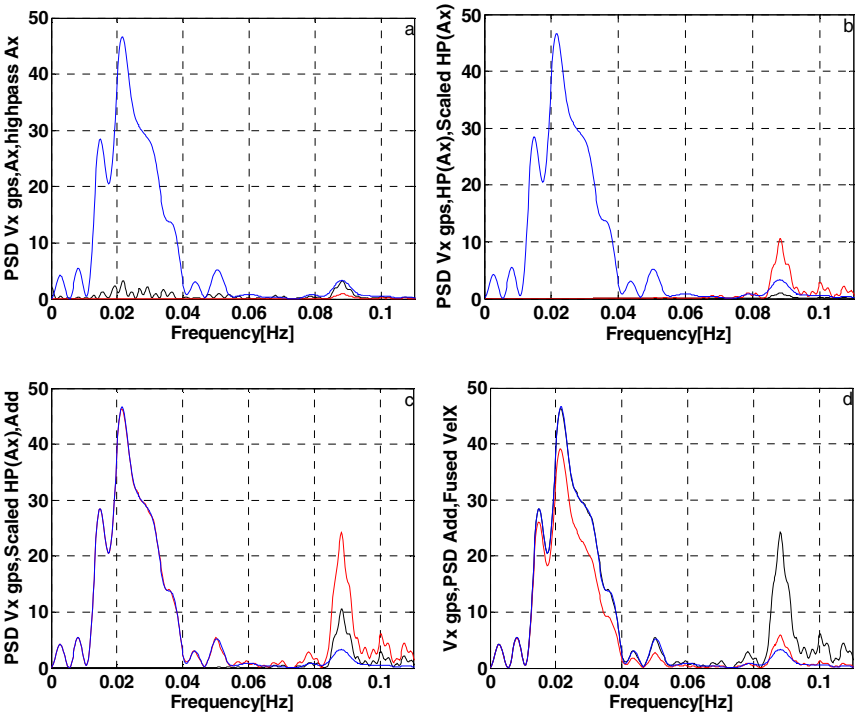

Fig. 52 PSD at particular steps of the data fusion process between the DGPS north component velocity and the IMU north component acceleration.

Figure 52 shows the Power Spectral Density (PSD) at key steps of the data fusion process between the DGPS north component velocity and the IMU north component acceleration. Figure 52a compares the DGPS north component velocity (blue), the north component of the IMU acceleration (black), and the same signal high-pass filtered (red). Figure 52b shows the DGPS north component velocity (blue) next to the high-pass filtered north component of the IMU acceleration (black), and the same signal scaled using the data fusion frequency (red). Figure 52c shows the DGPS north component velocity (blue), the scaled high-pass filtered IMU acceleration (black) and the addition of the two signals in red. The addition of scaled high-pass filtered IMU acceleration and the DGPS velocity is noted as a preemphasized signal. Finally Figure 52d shows the north component of the merged velocity (red) compare to the DGPS north component velocity (blue) and its addition to the scaled high-pass filtered IMU acceleration.

This study shows the high-pass filter applied to the raw acceleration measurement has reduced the region of frequency where the DGPS velocity spectrum has most of its significant spectral content (Figure 52.a) which allows the merged signal to follow the DGPS velocity spectrum before the data fusion frequency (Figure 52.d). Figure 52.b demonstrates the advantage of scaling the

acceleration signal, increasing the significant spectral content of the signal at higher frequencies where the DGPS signal is smothered by the noise. As a result, on Figure 52.c the preemphasized signal for frequencies smaller than the data fusion frequency (0.05Hz) comes predominantly from the DGPS velocity signal, while for frequencies greater than 0.05Hz the signal comes predominately from the IMU acceleration measurement. The enhanced version of the merged velocity is then retrieved by deconvolution using a 1st order Butterworth low-pass filter with a cutoff frequency at the data fusion point, 0.05Hz (Figure 52.d). The Butterworth filter is selected because typical and an Elliptic filter could also have been used.

The merged velocity signal is plotted in the time domain and compared to the direct integration of the IMU acceleration signal (Figure 53) to show the importance of the data fusion.

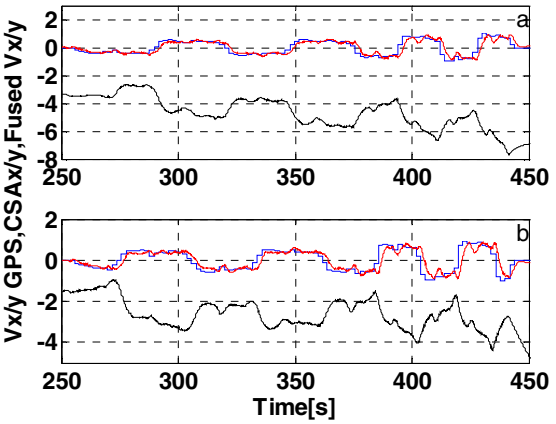

Fig. 53 Comparison in the time domain between the merged velocity (red) and the velocity obtained by direct integration of the raw IMU acceleration signal (black). The blue signal is the DGPS velocity measurement. The upper panel shows the north component of the signal (a) and the lower, the east component (b)

Now that the merged velocity estimate of the data acquisition system is available, the subsequent data fusion process applied is between the merged velocity and the DGPS position measurement to obtain a full frequency measure of the position estimate. The choice of the data fusion frequency is done in a similar fashion to aforementioned and the same data fusion point at 0.05Hz is selected. Figure 54 shows the diagram of the process of the second data fusion process between the enhanced velocity signal and the DGPS position measurement.

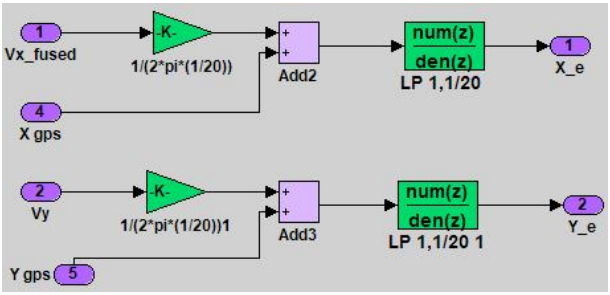

Fig. 54 Data fusion diagram between the DGPS position measurement and the merged velocity estimate obtained by fusing the IMU acceleration data and the DGPS velocity.

The enhanced (merged) velocity signals estimated from the previously described first data fusion process have most of their significant spectral content below the data fusion point from the DGPS velocity data. Therefore, the DGPS position signal and the enhanced velocity signal have matching spectra, below the data fusion point, and no pre-processing is needed on the DGPS velocity signal before the data fusion with the DGPS position data.

The next step is to verify the agreement between the DGPS position measurement and the merged position, as well as between the DGPS velocity measurement and the merged velocity at frequencies lower than the data fusion point.

4.2.3 Step 3: Low-Pass Filtering of the Merged and DGPS Data at the Data Fusion Frequency and Conclusion on Their Agreement Using the Crosscorrelation Method

To verify the agreement between the DGPS position (respectively velocity) measurements and the merged velocity estimates (respectively IMU acceleration) a 1st order Butterworth low-pass filter with a cutoff frequency at the data fusion point, 0.05Hz, is applied to both signals, which are then crosscorrelated. The Butterworth filter is selected because typical and an Elliptic filter could also have been used. During the square maneuver, the first crosscorrelation reveals the DGPS velocity signal and the merged velocity estimate agree by 99.02% for the north component (Figure 55.a) and by 99.01% for the east component (Figure 55.b). The second crosscorrelation reveals that the DGPS position signal and the merged position estimate agree by 99.58% for the north component (Figure 55.c) and by 99.59% for the east component (Figure 55.d).

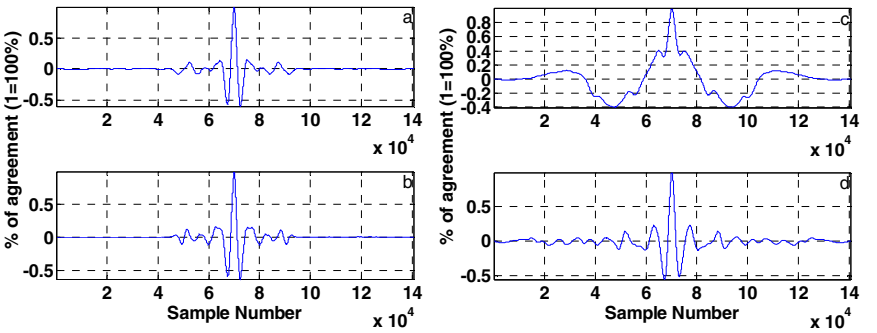

Fig. 55 Crosscorrelation (a) (respectively (b)) between the north, (respectively east) component of the DGPS velocity and the north (respectively east) component of the merged velocity estimates. Similarly, (c) (respectively (d)) corresponds to the crosscorrelation between the north (respectively east) component of the DGPS position and the north (respectively east) component of the merged position estimates.

Since the merged velocity of the data acquisition system is ultimately to be used to correct the ADCP data, it is important to estimate the standard deviation of that signal.

4.2.4 Step 4: High-Pass Filtering of the Merged Signals to Conclude on the Signals Standard Deviation

The standard deviation of the merged velocity error is typically determined by subtracting the expected velocity of the cart with the merged velocity estimate. However, since it was not possible to precisely control the motion of the cart, the expected velocity of the cart could not be determined. Instead, the estimation of the signals noise is applied by high-pass filtering the merged velocity signal, removing the motion of the vehicle, and computing the standard deviation of the filtered signal. Using this estimation process, the standard deviation of the merged velocity estimates (Table 8) is calculated for the three trajectories.

Table 8 Estimates of the standard deviation of the merged velocity signal for the three trajectories of the on shore data acquisition test.

Estimates of the merged velocity standard deviation [cm/s]	Square Path at 0.55m/s	Square Path at 0.93m/s	Square in zigzag course at 0.39m/s	Circle at 0.47m/s
NORTH COMPONENT	0.77	1.16	0.65	0.66
EAST COMPONENT	0.78	1.19	0.7	0.74

The standard deviation of the enhanced velocity signal averages 0.83 cm/s and the signal is used in the subsequent section for the correction of the ADCP data when performing a mission at sea.